

Spectral energy distributions of selfgravitating QSO discs

Edwin Sirko and Jeremy Goodman

Princeton University Observatory, Princeton, NJ 08544, USA

Received ??

ABSTRACT

We calculate spectral energy distributions (SEDs) of steady accretion discs at high accretion rates, as appropriate for bright QSOs, under the assumption that the outer parts are heated sufficiently to maintain marginal gravitational stability, presumably by massive stars formed within the disc. The SED is independent of the nature of these auxiliary sources if their inputs are completely thermalized. Standard assumptions are made for angular momentum transport, with an alpha parameter less than unity. With these prescriptions, the luminosity of the disc is sensitive to its opacity, in contrast to standard discs powered by release of orbital energy alone. Compared to the latter, our discs have a broader SED, with a second peak in the near-infrared that is energetically comparable to the blue bump. The energy in the second peak increases with the outer radius of the disc, provided that the accretion rate is constant with radius. By comparing our computed SEDs with observed ones, we limit the outer radius of the disc to be less than 10^5 Schwarzschild radii (R_S), or about one parsec, in a typical QSO. We also discuss some properties of our minimum- Q discs in the regions where auxiliary heating is dominant ($10^3 - 10^5 R_S$).

Key words: accretion discs–gravitation–quasars: general

1 INTRODUCTION

The standard theoretical paradigm for the central engine in quasars and their radio-quiet kin (QSOs) is a viscous accretion disc surrounding a massive black hole. Direct evidence for accretion discs, such as double-peaked emission lines (Eracleous & Halpern 1994), is important to seek but hard to come by. Perhaps the best reasons for belief in this paradigm are basic considerations of energy and angular momentum. Such discs are the most plausible astrophysical mechanism for converting rest mass to radiation with high efficiency, and if the relics of QSOs reside in galactic nuclei, then efficiencies $\gtrsim 10\%$ are required (Soltan 1982; Chokshi & Turner 1992; Yu & Tremaine 2002). On the other hand, the maximum specific angular momentum of a Kerr black hole, $GM/c \approx 1.4M_8 \text{ km s}^{-1}$, is far less than that of most mass in galaxies. ($M_8 = M/10^8 M_\odot$, where M is the mass of the black hole.) Accreting gas must be separated from its angular momentum, and a viscous disc is the most natural mechanism.

Most of the binding energy of the disc is in its inner parts, so that the outer radius of a standard accretion disc is almost irrelevant to its bolometric luminosity. In contrast, most of the angular momentum is in the outer regions, so that the outer radius of the disc is sensitive to the initial angular momentum of the gas that feeds it. In a previous paper (Goodman 2002, henceforth Paper I), it was argued that luminosity and angular momentum are coupled by the requirement that QSO discs be stable against their own self-gravity.

It is well known that gravitational stability is problematic in the outer parts of QSO discs (Shlosman & Begelman 1987). The threat to the standard paradigm is that a strongly selfgravitating disc is likely to fragment completely into stars, leaving insufficient gas to fuel the QSO. As discussed in Paper I, viable solutions to this difficulty fall into several categories:

- (i) enhanced angular momentum transport, not necessarily by viscous processes but at rates corresponding to a viscosity parameter $\alpha \gg 1$;
- (ii) auxiliary heating in excess of what is provided by dissipating orbital energy, so as to reduce the gas density and selfgravity of the disc;
- (iii) replacement of the outer disc with a very dense star cluster, whose collisional debris supply a disc of small radius and negligible selfgravity;

(iv) relatively low initial angular momentum for the gas, which therefore circularizes at small enough radius so as to avoid selfgravity.

A number of options in the first category were briefly considered in Paper I, including accretion driven by bars or global spiral waves (e.g. Shlosman & Begelman 1989) or by magnetized winds (e.g. Blandford & Payne 1982). But it was argued that none of these options is likely to achieve a supersonic accretion speed, and hence that discs cannot be stabilized much beyond one parsec by any of these mechanisms alone. The third category was tentatively rejected on the grounds that remnants of such star clusters are not observed in present day galactic nuclei. Recently, Pariev et al. (2002) have proposed discs whose thickness is supported primarily by magnetic pressure. If this is possible, it would imply lower disc densities on average, but the field might well squeeze the gas into dense clumps and thereby actually exacerbate selfgravity. At any rate, Pariev et al. (2002) do not apply their model to the cool outer regions beyond $10^3 R_S$.

The present paper will focus on some implications of the second category of solutions, which appear to be a natural compromise between a purely gaseous disc and a star cluster. It is reasonable to suppose that part of the gas fragments into stars, and that the energy released by nuclear fusion and other stellar processes (supernovae, stellar-mass black holes) may sufficiently heat the rest of the gas so as to prevent complete fragmentation (Collin & Zahn 1999a,b). There is a great deal of evidence that such a feedback cycle operates in the discs of spiral galaxies on kiloparsec scales.

Observed SEDs of typical quasars differ markedly from classical theoretical predictions in which the disc is assumed to be geometrically thin, optically thick, steady, and heated solely by viscous dissipation (Pringle 1981). To a first approximation, the typical SED is flat in a λF_λ plot over many decades in wavelength (Elvis et al. 1994). Relative to the classical predictions, there is excess emission at both X-ray and infrared wavelengths. The former is conventionally ascribed to comptonization in a hot corona at small radii (Shapiro et al. 1976), and the latter to passive reprocessing in warped or flared outer parts of the disc (Sanders et al. 1989).

We suppose that the infrared excess may be due to the energy inputs required to stabilize the outer disc against its own selfgravity. We obtain a lower bound on the auxiliary heating needed to stabilize the disc for given values of the macroscopic parameters: namely, the black hole mass (M), accretion rate (\dot{M}), and disc outer radius (r_{\max}). As shown in Paper I, and confirmed here with more realistic opacities, the inputs required for gravitational stability increase with the outer radius of the disc, r_{\max} . Paper I argued for an upper limit to r_{\max} based on the energy available from plausible sources, such as fusion or accretion onto stellar-mass black holes. In this paper, we find limits to r_{\max} from the SED.

It is not obvious that the auxiliary inputs should be completely thermalized, but if we assume this, then the SED can be predicted. The observed infrared emission of typical QSOs may be due largely to reprocessing of light emitted from the inner parts of the disc, as conventionally supposed. But by attributing all of the infrared light to the auxiliary energy inputs, and insisting that these inputs be sufficient for gravitational stability, we obtain bounds for r_{\max} . These bounds depend upon other parameters, especially the mass of the black hole, the accretion rate, and the viscosity parameter α . We explore these dependencies. The meaning of r_{\max} constrained by this method is the radius within which \dot{M} is sensibly constant; obviously the disc can be extended indefinitely if the accretion rate and mass at large radii are sufficiently small. Hence our limits on r_{\max} are best translated into upper limits on the initial angular momentum of the gas that is accreted.

The outline of our paper is as follows. §2 lays out the physical assumptions and governing equations for our disc models. These are the same as for the classical steady thin disc, with the one important exception that wherever the classical model would be gravitationally unstable, we invoke just enough auxiliary heating to stabilize it. A discussion of opacities becomes critically important, because the requirement of marginal stability fixes the density and temperature at the midplane (for given \dot{M} and α); the flux escaping from the disc, and hence the amount of auxiliary heating needed, then depend upon the optical depth. The computed radial structure of the disc is presented in §3 for parameters representative of bright quasars. Since our assumptions are no different from the classical ones at small radii, we emphasize the properties of our discs in the marginally selfgravitating region $r \gtrsim 10^3 R_S \sim 10^{-2}$ pc, and we compare our SEDs with those presented by Elvis et al. (1994) to obtain upper limits on the outer radius of the disc and the initial angular momentum of the gas. In the final section, we summarize our conclusions, issue the necessary caveats, and discuss directions for future research.

2 THE SELFGRAVITATING ACCRETION DISC MODEL

We start by considering the standard steady α disc. In this model, gas is accreted onto a central black hole of mass $M \sim M_S$ in a steady, Keplerian, geometrically thin accretion disc at a constant rate \dot{M} . Accretion is driven by viscous mechanisms, but the exact mechanism (probably magnetorotationally-driven turbulence) is unimportant here. Newtonian equations will be used. These are not accurate near the inner edge of the disc, but the effects of selfgravity are at large radii where relativistic corrections are unimportant.

We assume that each annulus of the disc radiates as a blackbody with temperature $T_{\text{eff}}(r)$. When accretion is the only source of thermal energy,

$$\sigma T_{\text{eff}}^4 = \frac{3}{8\pi} \dot{M}' \Omega^2, \quad (1)$$

where $\Omega = (GM/r^3)^{-1/2}$, and we have defined for notational simplicity $\dot{M}' = \dot{M}(1 - \sqrt{r_{\text{min}}/r})$ where r_{min} is the inner radius of the accretion disc. A zero-torque boundary condition has been assumed. In a relativistic thin-disc analysis, r_{min} would be the radius of the marginally stable orbit. In our newtonian framework, we set $r_{\text{min}} = R_S/4\epsilon$, where $R_S = 2GM/c^2$ is the Schwarzschild radius and $\epsilon \sim 0.1$ is the assumed radiative efficiency of accretion.

An α prescription for the viscosity is adopted, $\nu = \alpha c_s h \beta^b$, where $c_s = \sqrt{p/\rho}$ is the isothermal sound speed at the disc midplane, $h = c_s/\Omega$ the half thickness, and $\beta = p_{\text{gas}}/p$ is the ratio of gas pressure to total pressure at the midplane. The viscosity is related to the accretion rate by

$$\beta^b c_s^2 \Sigma = \frac{\dot{M}' \Omega}{3\pi \alpha}, \quad (2)$$

where $\Sigma = \int_{-\infty}^{+\infty} \rho dz$ is the surface density at a given radius. The parameter b is a switch that can be either 1, so that viscosity is proportional to gas pressure, or 0, so that viscosity is proportional to total pressure. Magnetic pressure is assumed to contribute negligibly to the thickness of the disc, even if magnetic stresses dominate angular momentum transport.

Because it will turn out that the optically thick assumption fails at large radii, we now turn to a study of the relationship between the midplane temperature T and T_{eff} . We assume radiative energy transport in the vertical (z) direction and write $\tau = \int_0^\infty \kappa \rho dz$ for the optical depth at the midplane. In the optically thick limit $\tau \gg 1$, the diffusive approximation is applicable so that $T^4 \sim \tau T_{\text{eff}}^4$, with a numerical factor of order unity that depends upon the vertical variation of opacity κ and the vertical distribution of viscous dissipation. The latter is not yet predictable from theory, despite major advances in understanding magnetohydrodynamic disc turbulence. If one assumes constant dissipation per unit optical depth, then

$$T^4 \approx \left(\frac{3}{8}\tau + \frac{1}{2} \right) T_{\text{eff}}^4,$$

where the “+1/2” follows from the Eddington approximation to the boundary condition at the photosphere. In the opposite limit of low optical depth, the radiative flux from one side of the disc scales as $\sigma T_{\text{eff}}^4 \sim \tau \sigma T^4$. Again a numerical factor occurs. One should distinguish between absorption and scattering opacity, but at the large accretion rates of interest to us, optically thin conditions tend to occur where the opacity is primarily absorptive. For a vertically isothermal disc, $\sigma T_{\text{eff}}^4 = 4\tau \sigma T^4$ when $\tau \ll 1$. Simple interpolation between the optically thin and optically thick limits yields eq. (4) below, which satisfies the physical requirement that $T_{\text{eff}} \leq T$ for any τ (in fact, the minimum of T^4/T_{eff}^4 is 1.112 and occurs when $\tau = \sqrt{2/3}$).

We represent the effective radiation pressure by eq. (7). In the optically thick case, in view of eq. (4), this reduces to the usual $p_{\text{rad}} = aT^4/3$ relation, but in the optically thin case, $p_{\text{rad}} \rightarrow 2\tau^2 \sigma T^4/c$: one power of τ represents the inefficiency with which photons are radiated, and the second is the fraction of these photons that transfer their momentum to the gas, thereby helping to support the thickness of the disc. The numerical factor is correct for an isothermal slab of midplane optical depth $\tau \ll 1$.

We also must know the opacity in the disc (equation 13). We use the opacity tables of Iglesias & Rogers (1996) for high temperatures and those of Alexander & Ferguson (1994) for low temperatures, with $X = .70$, $Z = .03$. Figure 1 illustrates the opacity as a function of density and temperature. The two opacity tables overlap in the region $3.75 < \log T < 4.1$, and Figure 1 demonstrates their agreement. Additionally, the loci of two disc models are projected onto the plot. Extrapolation of the opacity tables in the low density regime is necessary. This is done by simply assigning κ its value at the low-density edge of the opacity table (using the same value of T). This extrapolation is presumably correct for high temperatures ($T \gtrsim 10^4$ K) where the opacity is dominated by electron scattering. At lower temperatures, the extrapolation is less certain, but we feel it is reasonable as a first approximation. Also, for $\log T < 3$, κ is assigned its value at the low-temperature edge of the opacity table, which is approximately $10^{0.76} \text{ cm}^2 \text{ g}^{-1}$.

In summary, our governing equations for the disc are as follows (we take $m = .62 m_H$ as the mean molecular mass):

$$\sigma T_{\text{eff}}^4 = \frac{3}{8\pi} \dot{M}' \Omega^2 \quad (3)$$

$$T^4 = \left(\frac{3}{8}\tau + \frac{1}{2} + \frac{1}{4\tau} \right) T_{\text{eff}}^4 \quad (4)$$

$$\tau = \frac{\kappa \Sigma}{2} \quad (5)$$

$$\beta^b c_s^2 \Sigma = \frac{\dot{M}' \Omega}{3\pi \alpha} \quad (6)$$

$$p_{\text{rad}} = \frac{\tau \sigma}{2c} T_{\text{eff}}^4 \quad (7)$$

$$p_{\text{gas}} = \frac{\rho k T}{m} \quad (8)$$

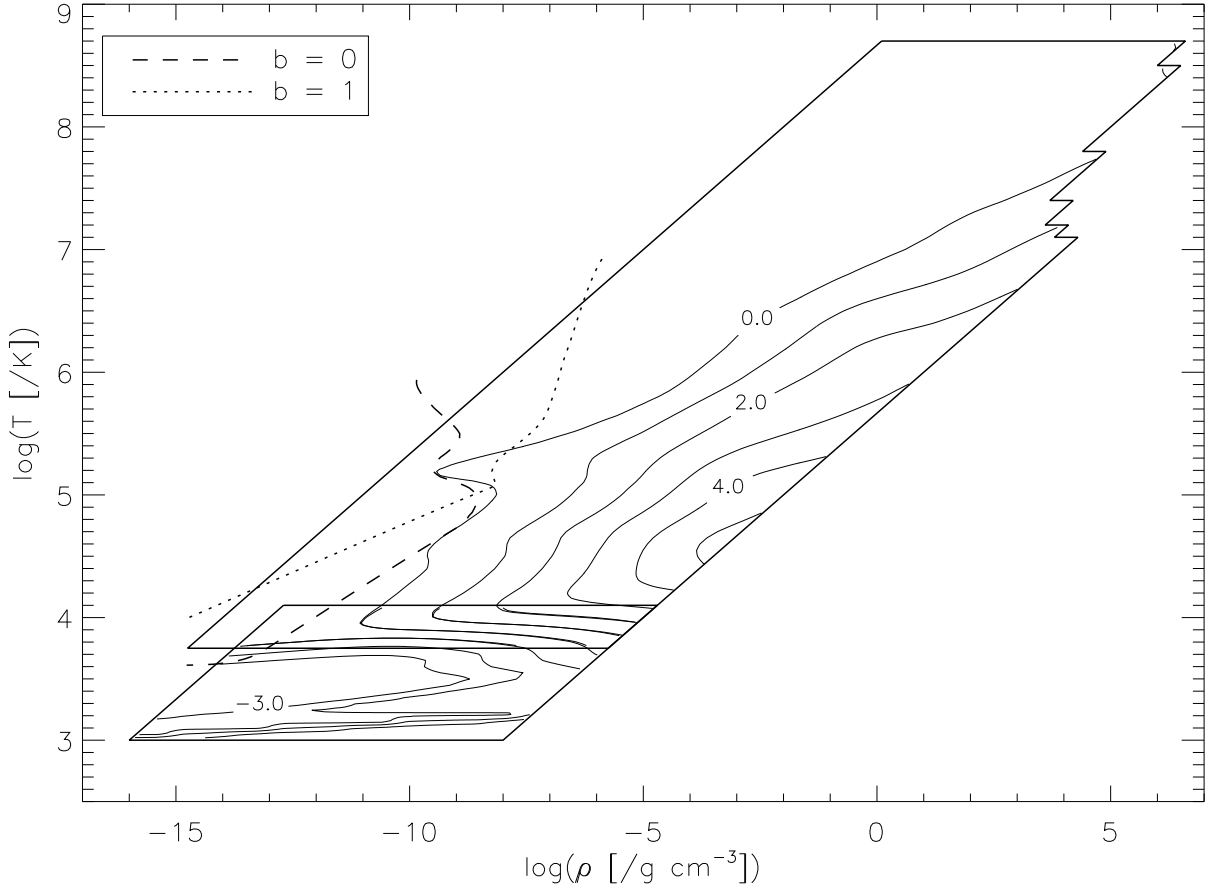


Figure 1. Contour plot of opacity as a function of density and temperature, as provided by Iglesias & Rogers (1996) (high- T region) and Alexander & Ferguson (1994) (low- T region) for $X = .70$, $Z = .03$. Contours represent integer values of the logarithm of the opacity ($\text{cm}^2 \text{g}^{-1}$). The overlap region $3.75 < \log T < 4.1$ is plotted with contours from both sources; their agreement is illustrated. The dashed ($b = 0$) and dotted ($b = 1$) lines show trajectories of (ρ, T) for typical examples of our disc models (Figure 2 for $b = 0$), up to $r_{\text{max}} = 10^5 R_{\text{S}}$.

$$\beta = \frac{p_{\text{gas}}}{p_{\text{gas}} + p_{\text{rad}}} \quad (9)$$

$$\Sigma = 2\rho h \quad (10)$$

$$h = \frac{c_s}{\Omega} \quad (11)$$

$$c_s^2 = \frac{p_{\text{gas}} + p_{\text{rad}}}{\rho} \quad (12)$$

$$\kappa = \kappa(\rho, T) \quad (13)$$

For an accretion disc with given parameters M , \dot{M} , α , and b , we can solve these eleven equations for the eleven unknowns: T_{eff} , T , τ , Σ , β , c_s , p_{rad} , p_{gas} , ρ , h , and κ at every radius r , which is related simply to Ω .

The outer parts of the accretion disc will be prone to selfgravity if Toomre's stability parameter,

$$Q \equiv \frac{c_s \Omega}{\pi G \Sigma} \approx \frac{\Omega^2}{2\pi G \rho} \quad (14)$$

is $\lesssim 1$. In our model, we assume there is some feedback mechanism, perhaps star formation, that supplies just enough additional heat to the disc as to prevent Q falling below a minimum value $Q_{\text{min}} \approx 1$. The energy source for these auxiliary inputs must be something other than the orbital energy of the gas, for example, nuclear fusion in stars. The quantity of these inputs is fixed by the properties of the disc: in particular the opacities, since the more easily radiation escapes, the more the disc must be heated to maintain stability. The nature of the auxiliary sources is not important to the spectral energy distribution as long as their inputs are completely thermalized.

When $Q = Q_{\min}$, eq. (3), which assumes the disc to be heated by release of orbital energy only, is no longer appropriate; we replace it with

$$\rho = \frac{\Omega^2}{2\pi G Q_{\min}} \quad (15)$$

and T_{eff} must be obtained from equation 4.

Once T_{eff} is known as a function of r , we compute a theoretical spectral energy distribution for the disc as a weighted sum of Planck functions:

$$L_{\lambda} = \frac{2hc^2}{\lambda^5} \int_{r_{\min}}^{r_{\max}} 2\pi r dr \frac{1}{\exp[hc/\lambda k T_{\text{eff}}(r)] - 1} \quad (16)$$

This formula does not allow for differences between effective and color temperature. Such differences are most likely in those parts of the disc whose emission is dominated by passive reprocessing (Sanders et al. 1989) or are optically thin (to absorption). In fact we find that much of the auxiliary heat input occurs in regions that are marginally optically thick, since these regions cool most efficiently. We feel that eq. (16) is adequate for a first investigation: it may somewhat overestimate the wavelength of the infrared peak associated with the auxiliary heating, but the area under the peak should be roughly correct.

3 RESULTS

We define $l_E \equiv L_0/L_E$, where $L_0 \equiv \epsilon \dot{M} c^2$ is the luminosity corresponding to a nonselfgravitating (i.e., with no auxiliary heating) disc with accretion rate \dot{M} , and L_E is the Eddington luminosity. In our models we always set $\epsilon = .1$ and $Q_{\min} = 1$.

The radial structure of a typical accretion disc ($M_8 = 1$, $l_E = .5$, $\alpha = .01$) is presented in Figure 2 for $b = 0$. The outer radius of $r_{\max} = 10^7 R_S$ will be shown to be unrealistic, but this model illustrates several key regimes in the disc.

The inner region ($2.5 \lesssim r/R_S \lesssim 10^2$) is radiation dominated ($\beta \ll 1$) and the temperature is high enough to ensure that the opacity is dominated by electron scattering, hence constant. In view of equation 1, $T_{\text{eff}} \propto r^{-3/4}$. When Q would otherwise drop below 1 (here, at $r \approx 10^3 R_S$), we hold Q constant, which ensures that $\rho \propto r^{-3}$. In this auxiliary heating region, if $\kappa = \text{constant}$, then $T_{\text{eff}} \propto r^{-3/8}$. After the disc becomes optically thin ($\tau < 1$) we find multiple solutions. The one with the least optical depth corresponds to the continuous line in all panels; it reaches constant T and κ . There is an optically thick solution with $T \propto r^{-3/4}$. Since the region in which we find multiple solutions is so dependent on the extrapolation of opacity into low-density and low-temperature regimes, the interpretation must be approached with caution. However, the presence of multiple solutions raises the possibility of thermal instability and time-dependence (see, for example, Siemiginowska et al. 1996). Note that in our solutions, \dot{M} is constrained to be constant throughout the disc. Several of the panels in Fig. 2 contain only one curve in the region of multiple solutions ($r \gtrsim 10^5$ pc): this is because ρ and c_s are uniquely determined by r , \dot{M} , α , and Q *via* eqs. (15) and (6) when $b = 0$.

For $b = 1$, the effective temperature has the same $T_{\text{eff}} \propto r^{-3/4}$ behavior in the inner part of the disc, but differs from the $b = 0$ case in the auxiliary heating region. For $\kappa \propto \text{constant}$ in this region, in the optically thick solution, $T \propto r^{-1/2}$ & $T_{\text{eff}} \propto r^{-1/4}$, and in the optically thin case, $T \propto \text{const.}$ & $T_{\text{eff}} \propto r^{-3/8}$.

The calculated SED of this typical model is presented in Figure 3, for outer radii of $r_{\max} = 10^3, 10^4, 10^5, 10^6$, and $10^7 R_S$. (All of our SEDs assume that the disc is viewed face-on.) Since T_{eff} may have multiple solutions in certain regions of the disc, the SEDs are plotted as bounded regions with the top (bottom) boundary corresponding to the largest (least) T_{eff} . Also plotted is the arbitrarily normalized mean energy distribution (MED) from 47 observed quasars (Elvis et al. 1994). The authors caution that the dispersion about this mean is large, of order ‘‘one decade for both the infrared and ultraviolet components when the MED is normalized at $[\lambda = 1.25 \mu\text{m}]$.’’ The $r_{\max} = 10^3 R_S$ case has an expected $\lambda f_{\lambda} \propto \lambda^{-4/3}$ behavior since selfgravity is not an issue. Relativistic effects (Laor & Netzer 1989; Sun & Malkan 1989) only influence the SED at and blueward of the short wavelength peak, since this emission comes from the innermost parts of the disc.

Figure 4 shows the dependence of the infrared bump on the mass of the central black hole. (Note that the wavelength corresponding to the blue bump has an expected $M^{1/4}$ dependence.) The Eddington ratio as defined above is kept constant at $l_E = .5$: note that this parameter defines \dot{M} rather than the total luminosity of the disc, which includes the auxiliary heat inputs. In the top two panels, r_{\max} is set to $10^5 R_S$, and the relative prominence of the infrared bump grows with M because the reduced radius at which $Q_{\min} = 1$ decreases with M (Paper I). The bottom two panels have r_{\max} fixed at 1 pc; here larger values of M tend to reduce the infrared bump. This dependence is illustrated in Figure 7. Solutions for the disc are considered incompatible with the observations if λf_{λ} at the maximum of the infrared bump is more than ten times that of the blue bump.

Figure 5(a) shows that while the blue bump increases with mass accretion rate, the energy output of the infrared bump is hardly affected, for the $b = 0$ case. This invariance is caused by two competing factors as \dot{M} is increased: T_{eff} is higher in the selfgravitating region, but because T is also higher, the onset of the optically thin regime, and thus a sharp increase in T_{eff} as shown in Figure 2, is delayed. Similar considerations explain the behavior of the infrared bump in Figure 5(b), for

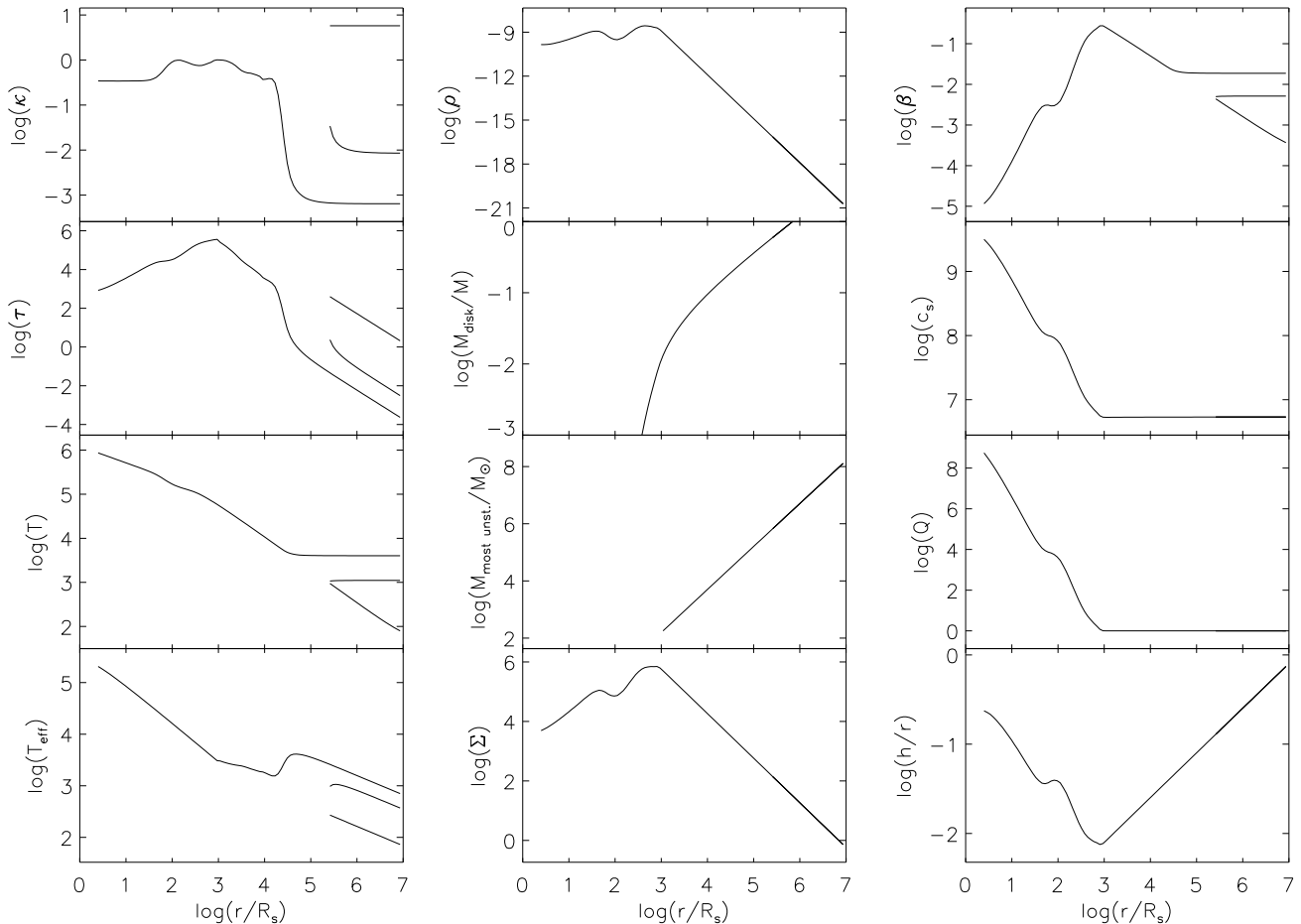


Figure 2. Dependence of an assortment of parameters on radius for our $b = 0$ (*i.e.*, viscosity \propto total pressure) canonical case of $M_8 = 1$, $l_E = .5$, $\alpha = .01$, and $Q_{\min} = 1$. All units are in cgs except for those represented as reduced variables. The integrated disc mass $\int_{r_{\min}}^r 2\pi r' \Sigma dr'$ is in units of the central black hole mass M , but the most unstable mass $c_s^4/G^2\Sigma$ is in units of solar masses. The SED for this model is the vertically-hatched region in Figure 3(a).

$b = 1$. For low accretion rates, the midplane temperature drops low enough that the disc becomes optically thin before the end of the disc (at $r_{\max} = 10^5 R_S$), which drives up T_{eff} .

In Figure 6, the same argument explains the behavior of the infrared bump in both the $b = 0$ and $b = 1$ cases. The onset of the optically thin selfgravitating region is at smaller radii with increasing α for both cases, but T_{eff} is higher in the optically thick selfgravitating region for $b = 1$.

It is clear that additional heating in the outer parts of our accretion discs results in a second bump in the SED. Assuming that this outer-disc contribution to the SED can be no more prominent than infrared emission in the observed MED, we can already place tight constraints on the outer radius of these disc models: $r_{\max} \lesssim 10^4 - 10^5 R_S \sim 0.1 - 1$ pc.

4 SUMMARY AND DISCUSSION

We have estimated spectral energy distributions (SEDs) of bright QSOs using standard assumptions, with one addition: where the disc would otherwise be gravitationally unstable, we have postulated additional sources of heat, other than release of orbital energy by accretion, just sufficient to maintain gravitational stability. These sources become necessary beyond $\sim 10^3 R_S$ for typical parameters. Assuming their energy inputs to be locally and completely thermalized, we have calculated their contribution to the SED and luminosity of the disc, which occurs primarily in the red and near infrared. The larger the disc, the more auxiliary heating is required. For typical black-hole masses and accretion rates inferred from the blue bump, the auxiliary inputs actually exceed the power derived from accretion if the disc extends beyond $10^4 - 10^5 R_S$, or about one parsec. This would be incompatible with the typical SED of bright QSOs, which is approximately flat in λF_λ .

Paper I placed similar limits on r_{\max} from energetic arguments. It was assumed that the stars or small black holes that heat the disc also form within the disc, and that the mass in these objects is at most comparable to that of the disc. The

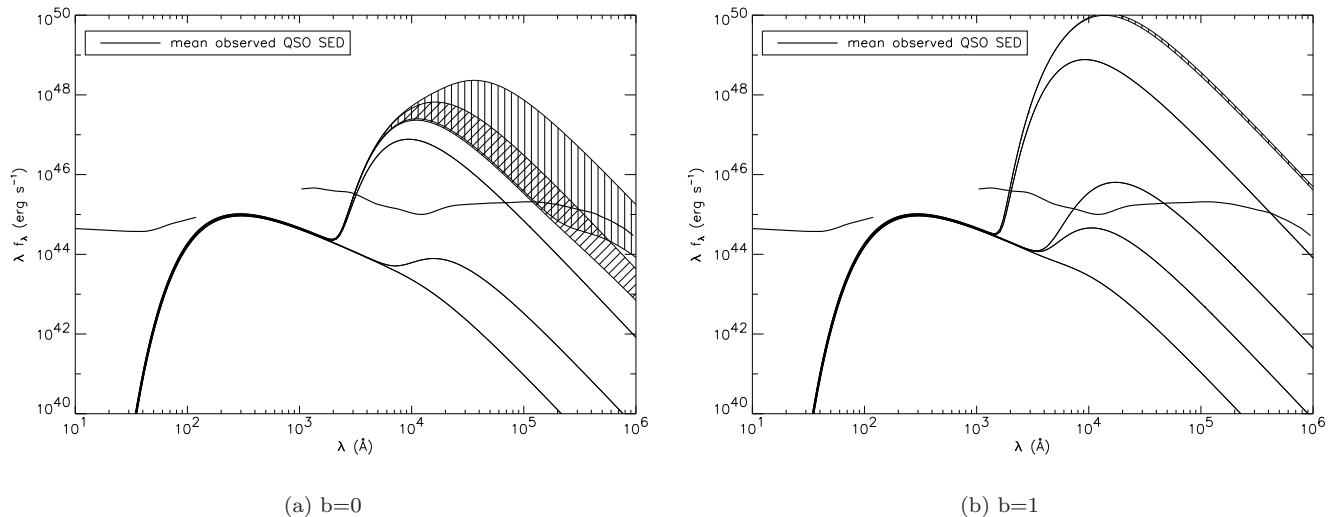


Figure 3. Calculated spectral energy distributions for our accretion disc models with $M_8 = 1$, $l_E = .5$, $\alpha = .01$. The five SEDs, in order of increasing total luminosity, correspond to the five values of $r_{\max}/R_S = 10^3, 10^4, 10^5, 10^6$ (diagonally-hatched), and 10^7 (vertically-hatched). Multiple solutions for $T_{\text{eff}}(r)$ are responsible for the ambiguity of the SEDs plotted as bounded regions.

present limits do not rely on these assumptions. That is to say, if the disc were heated by a much larger mass in stars, the limits of Paper I could be relaxed, but those based on the SED would still apply.

It has been assumed that the accretion rate is constant with radius, so that \dot{M} at large radii can be derived from the luminosity in the blue bump (which has no contribution from the auxiliary sources). If \dot{M} at $r \gtrsim 1$ pc is several orders of magnitude less than it is at $r \lesssim 10^3 R_S$, then the disc could be much more extensive than we have supposed. The Stefan-Boltzmann law implies that the observed luminosity at 10μ must in any case come from $r \gtrsim 2(\lambda L_\lambda / 10^{46} \text{ erg s}^{-1})^{1/2}$ pc, but this does not require that the surface density at that distance is as high as in a constant- \dot{M} disc. Therefore, it is useful to rephrase the limits in terms of the initial angular momentum of the gas supplied to the disc. At least on a time average, \dot{M} should be constant inside the radius corresponding to the initial angular momentum. The relationship is

$$J_0 \approx 660 (r_{\text{pc}} M_8)^{1/2} \text{ pc km s}^{-1}. \quad (17)$$

This is quite small compared with the product of virial velocity ($\sim 300 \text{ km s}^{-1}$) and scale size ($\sim 1 \text{ kpc}$) of QSO hosts, and it may be important to ask where gas with such low angular momentum comes from. Furthermore, the mass of a gravitationally stable disc that obeys our constraints on the SED is generally much less than that of the black hole, so that the disc must be replenished many times over to grow the black hole by accretion.

Our treatment of the disc is highly simplified and certainly crude compared with many past efforts. We have ignored relativistic effects, adopted a one-zone model for the vertical structure, used Rosseland mean opacities without distinguishing between scattering and absorption, taken a constant molecular weight, and represented angular-momentum transport by the usual viscous α prescription. We feel that these simplifications are justified by the strong dependence of the auxiliary inputs and the SED on the outer radius of the disc. A more detailed treatment of the physics that one actually understands seems unlikely to change our conclusions concerning r_{\max} . Radical enhancements in transport (equivalent to $\alpha \gg 1$), or magnetic pressures $\gg p_{\text{gas}}$ (as suggested by Pariev et al. 2002) could make some difference, but these are not yet understood.

Despite what has just been said, a more elaborate treatment of vertical structure and radiative transfer might point to a redistribution of the auxiliary energy inputs in wavelength, if not their total contribution to the disc luminosity. Unfortunately, one has no reliable predictions for the vertical distribution of purely viscous heating, much less of the auxiliary sources postulated here, which will limit the credibility of detailed vertical models.

Even if the actively accreting parts of QSO discs are smaller than 0.1 pc, it is still possible that selfgravity is important in them, and therefore that they form stars. Quiescent galactic nuclei with black holes, even in early-type galaxies, often show kinematic evidence of compact stellar discs (Gebhardt et al. 2000; Bower et al. 2001; de Zeeuw et al. 2002). Nuclear starbursts (albeit on scales $\sim 10^2$ pc) are usually accompanied by AGN activity (Sanders 1999; Heckman 1999). The black hole in our own Galaxy, though not an AGN and estimated to have a very low accretion rate (Quataert et al. 1999), is surrounded by what appear to be young high-mass stars at $r \lesssim 0.1$ pc (Krabbe et al. 1995). More theoretical attention should be paid to star formation in these extreme environments, where the densities, temperatures, and tidal fields are much higher than in normal giant molecular clouds.

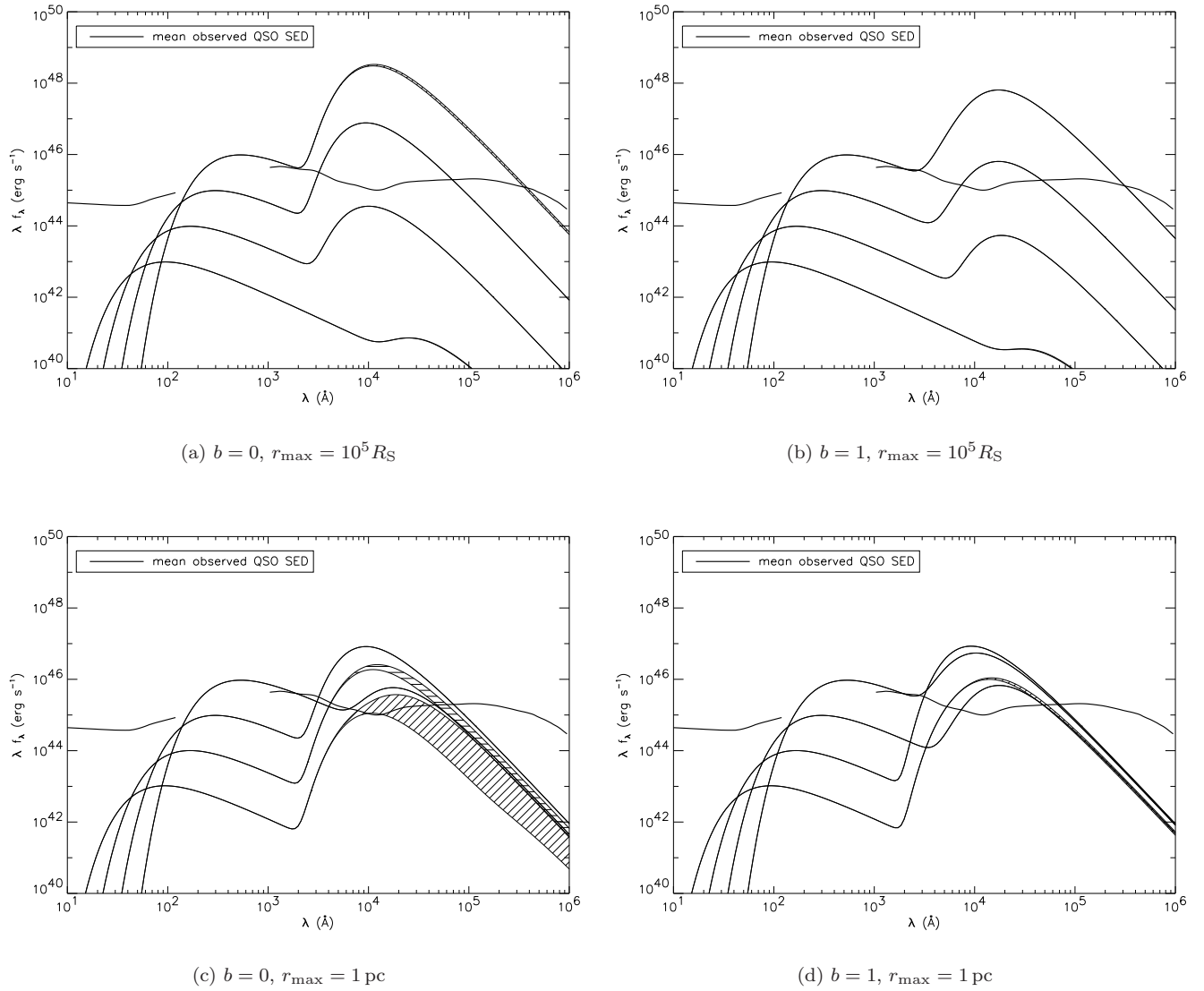


Figure 4. SEDs for the models with $l_E = .5$, $\alpha = .01$. The four SEDs shown here, in order of increasing blue bump, correspond to $\log M_8 = -2, -1, 0, 1$. The outer radius is set to $r_{\max} = 10^5 R_S$ in the top two panels, but it is fixed at $r_{\max} = 1 \text{ pc}$ in the bottom two panels. Compare the bottom two panels to Figure 7.

We thank Iskra Strateva and Jonathan Tan for helpful discussions.

REFERENCES

- Alexander D. R., Ferguson J. W., 1994, *ApJ*, 437, 879
 Blandford R. D., Payne D. G., 1982, *MNRAS*, 199, 883
 Bower G. A., Green R. F., Bender R., Gebhardt K., Lauer T. R., Magorrian J., Richstone D. O., Danks A., Gull T., Hutchings J., Joseph C., Kaiser M. E., Weistrop D., Woodgate B., Nelson C., Malumuth E. M., 2001, *ApJ*, 550, 75
 Chokshi A., Turner E. L., 1992, *MNRAS*, 259, 421
 Collin S., Zahn J., 1999a, *A&A*, 344, 433
 Collin S., Zahn J., 1999b, *Ap&SS*, 265, 501
 de Zeeuw P. T., Bureau M., Emsellem E., Bacon R., Marcella Carollo C., Copin Y., Davies R. L., Kuntschner H., Miller B. W., Monnet G., Peletier R. F., Verolme E. K., 2002, *MNRAS*, 329, 513
 Elvis M., Wilkes B. J., McDowell J. C., Green R. F., Bechtold J., Willner S. P., Oey M. S., Polonski E., Cutri R., 1994, *ApJS*, 95, 1

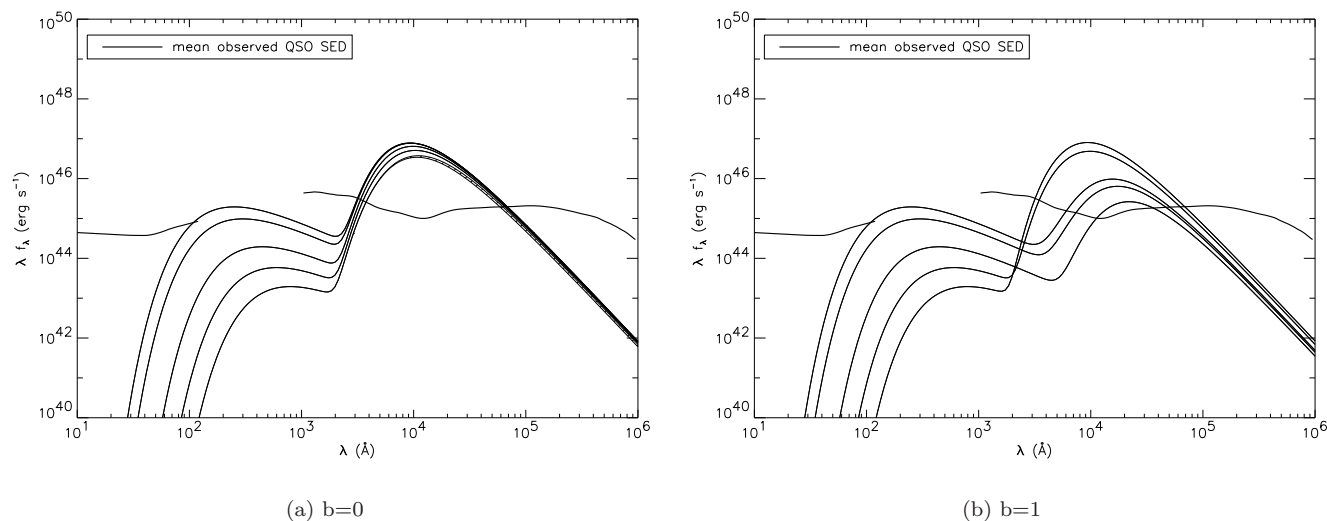


Figure 5. SEDs for the models with $M_8 = 1$, $\alpha = .01$, $r_{\max} = 10^5 R_S$. The five SEDs shown here, in order of increasing blue bump, correspond to $l_E = .01, .03, .1, .5, 1$.

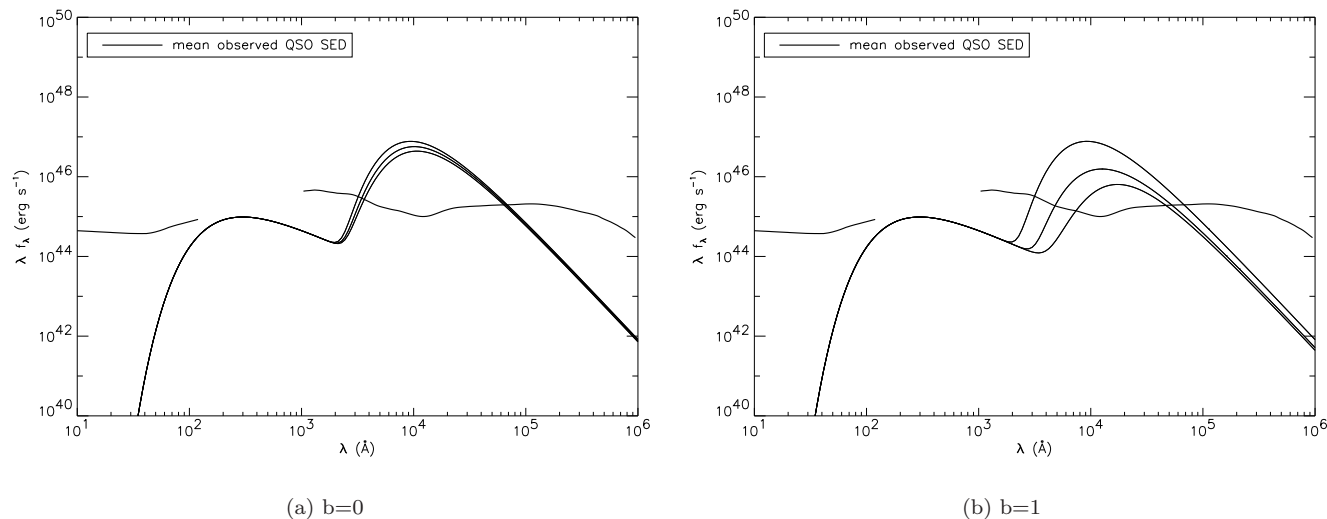


Figure 6. SEDs for the models with $M_8 = 1$, $l_E = .5$, $r_{\max} = 10^5 R_S$. The three SEDs shown here, in order of decreasing (increasing) infrared bump for $b = 0$ ($b = 1$), correspond to $\alpha = .01, .1, .3$.

- Eracleous M., Halpern J. P., 1994, ApJS, 90, 1
 Gebhardt K., Richstone D., Kormendy J., Lauer T. R., Ajhar E. A., Bender R., Dressler A., Faber S. M., Grillmair C., Magorrian J., Tremaine S., 2000, AJ, 119, 1157
 Goodman J., 2002, astro-ph/0201001
 Heckman T. M., 1999, in IAU Symp. 193: Wolf-Rayet Phenomena in Massive Stars and Starburst Galaxies Vol. 193, The energetic role of massive stars in the AGN phenomenon. pp 703–715
 Iglesias C. A., Rogers F. J., 1996, ApJ, 464, 943
 Krabbe A., Genzel R., Eckart A., Najarro F., Lutz D., Cameron M., Kroker H., Tacconi-Garman L. E., Thatte N., Weitzel L., Drapatz S., Geballe T., Sternberg A., Kudritzki R., 1995, ApJ, 447, L95
 Laor A., Netzer H., 1989, MNRAS, 238, 897
 Pariev V. I., Blackman E. G., Boldyrev S. A., 2002, astro-ph/0208400
 Pringle J. E., 1981, ARAA, 19, 137
 Quataert E., Narayan R., Reid M. J., 1999, ApJ, 517, L101

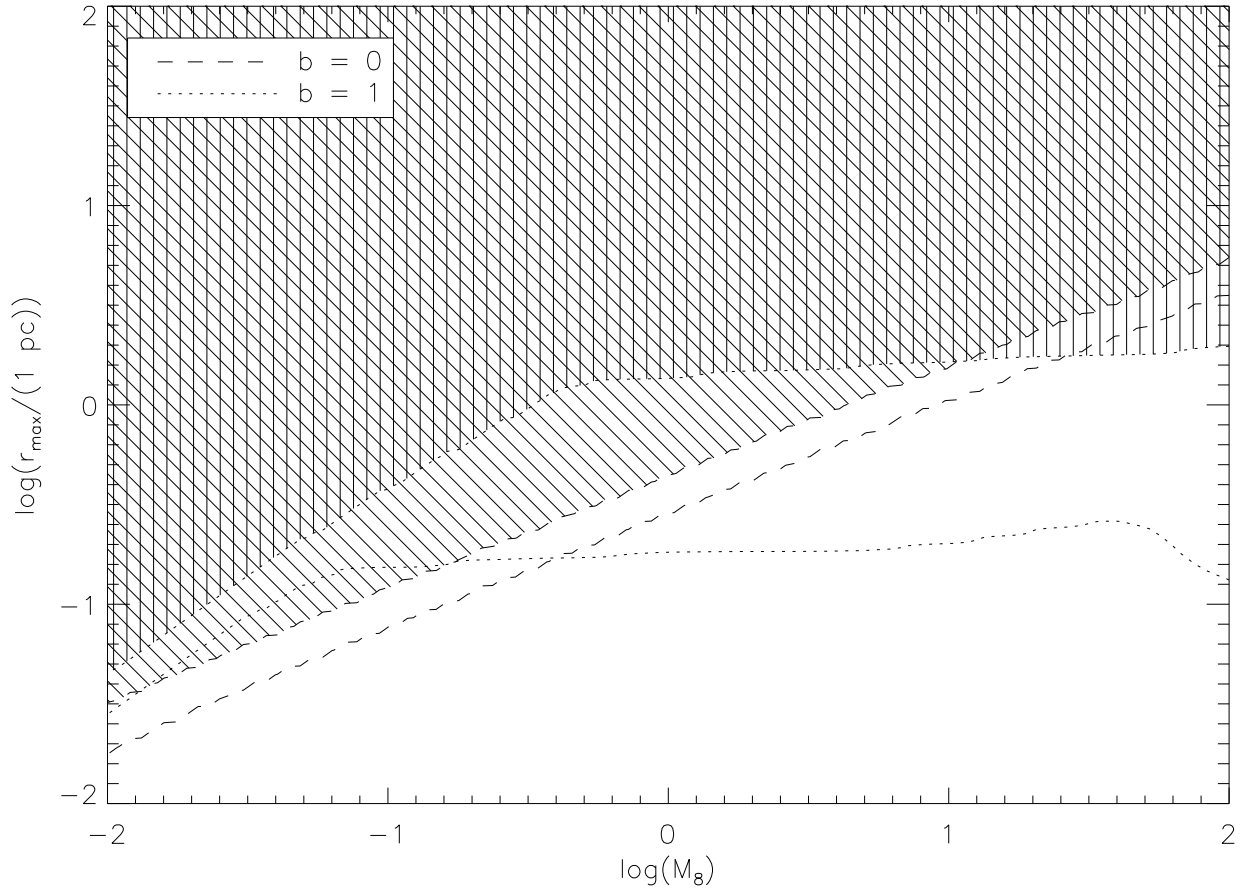


Figure 7. Locus of allowable (M, r_{\max}) , with $l_E = .5$ and $\alpha = .01$ fixed. The bottom dashed (dotted) contour represents solutions for $b = 0$ ($b = 1$) for which $(\lambda f_\lambda)_{\text{IR bump}} / (\lambda f_\lambda)_{\text{blue bump}} = 1$, and the top contour represents solutions for which $(\lambda f_\lambda)_{\text{IR bump}} / (\lambda f_\lambda)_{\text{blue bump}} = 10$. Thus, the diagonally-hatched region is the observationally-constrained approximate forbidden region for $b = 0$, and the vertically-hatched region is the forbidden region for $b = 1$. In both cases r_{\max} is forbidden to be much larger than ~ 1 pc.

Sanders D. B., 1999, Ap&SS, 266, 331

Sanders D. B., Phinney E. S., Neugebauer G., Soifer B. T., Matthews K., 1989, ApJ, 347, 29

Shapiro S. L., Lightman A. P., Eardley D. M., 1976, ApJ, 204, 187

Shlosman I., Begelman M. C., 1987, Nature, 329, 810

Shlosman I., Begelman M. C., 1989, ApJ, 341, 685

Siemiginowska A., Czerny B., Kostyunin V., 1996, ApJ, 458, 491

Soltan A., 1982, MNRAS, 200, 115

Sun W., Malkan M. A., 1989, ApJ, 346, 68

Yu Q., Tremaine S., 2002, MNRAS, 335, 965